Supporting Information

A Thiophene-based and Sulfur-enriched Highly Conjugated Hyper-Crosslinked Polymer for Efficient Sequestration of Iodine from Various Media

Sk Abdul Wahed, Mustafa Maqbool, Atikur Hassan*, and Neeladri Das*

Department of Chemistry, Indian Institute of Technology Patna, Patna, Bihar-800106, India

Corresponding Authors E-mail: atikurhassan@gmail.com, neeladri@iitp.ac.in or neeladri2002@yahoo.co.in

Contents

Section-1

General Characterization and Physical Measurements:

Fourier transform infrared spectra (FT-IR) of samples were collected using the ATR mode of a PerkinElmer 400 FT-IR spectrophotometer. Solid-state ^{13}C-NMR spectrum of Bi-Thio HCP was recorded with 500 MHz JEOL NMR instrument. The PXRD patterns were obtained using a Panalytical XRD using Cu Kα radiation (α =1.5406 Å), with a scan speed of 2°/min. Thermogravimetric analysis (TGA) of Bi-Thio HCP samples were performed by using a Perkin Elmer STA 6000 analyser. The experiments were carried out in the temperature range of 30−800 °C, under nitrogen atmosphere with regulated heating rate of 10°C/min. The porous nature of the polymer and its surface area were determined using Quantachrome Autosorb iQ2 instrument (Quantachrome, USA). Prior to analysis, a given sample was activated at 120 °C for 24h. Following activation, the sample was subjected to gas adsorption measurements (P/P_0 range from 0 to 1 atm.) at 77 K. Quantachrome ASiQwin Version 3.01 software was used for the data analyses. The Brunauer-Emmett-Teller (BET) model was used for the calculation of the specific surface area of Bi-Thio HCP. The distribution of pore size was obtained from the nitrogen gas sorption curves (recorded at 77 K) and utilizing the non-local density functional theory (NL-DFT). UV-visible absorption spectra were recorded on a Shimadzu UV-2550 UV-vis spectrophotometer. Morphological studies were done using a ZEISS Field Emission Scanning Electron Microscope (FE-SEM). Before analysis, the samples were sputter-coated with gold. A voltage of 20 kV was applied to perform elemental analyses and mapping with energy dispersive elemental analysis technique (EDX). The CHNS elemental composition was determined using an Elementar vario MICRO Cube instrument. Raman spectrum was obtained using a laser of 532 nm on a Renishaw Ramanscope system (micro-Raman spectrometer). All the digital images reported herein were captured using OnePlus Nord CE 2 Lite mobile camera.

Section-2

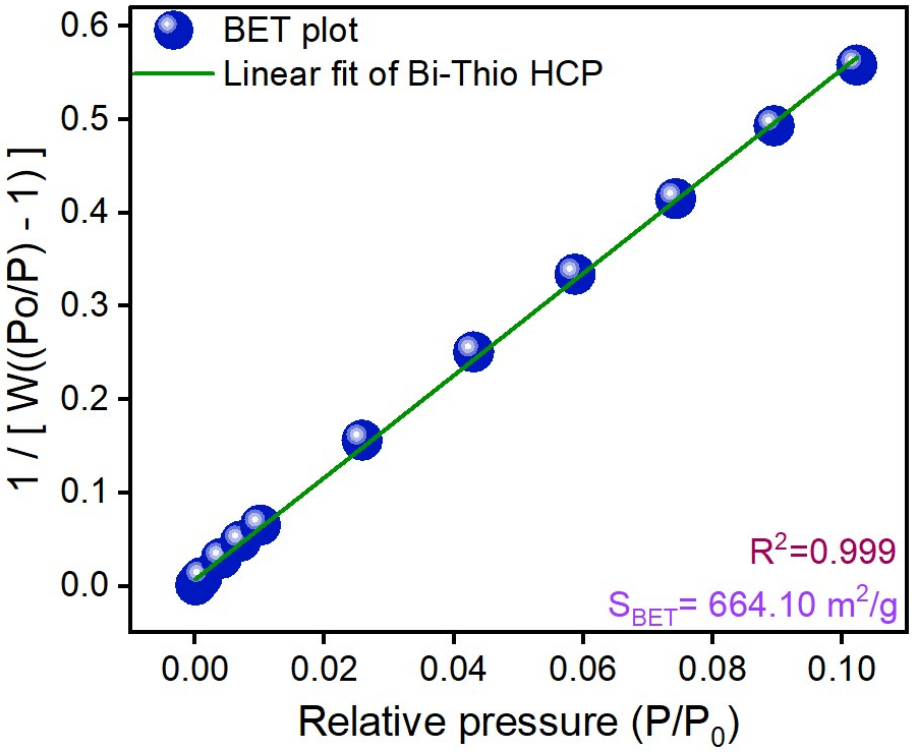

Figure S1: BET plot of Bi-Thio HCP

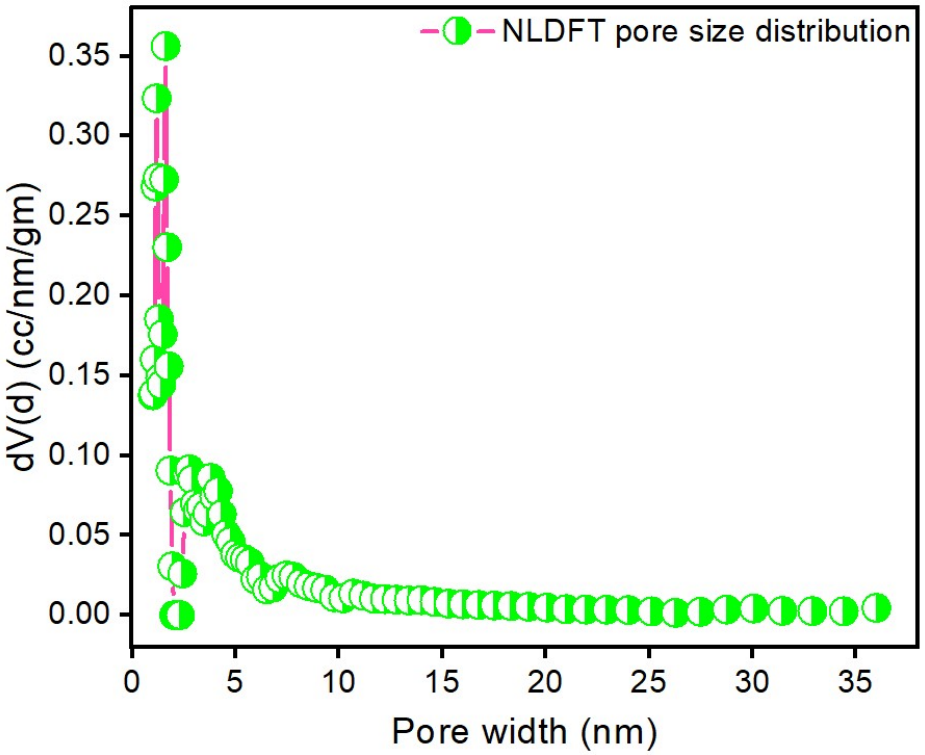

Figure S2: The pore size distribution of Bi-Thio HCP by using the NLDFT method

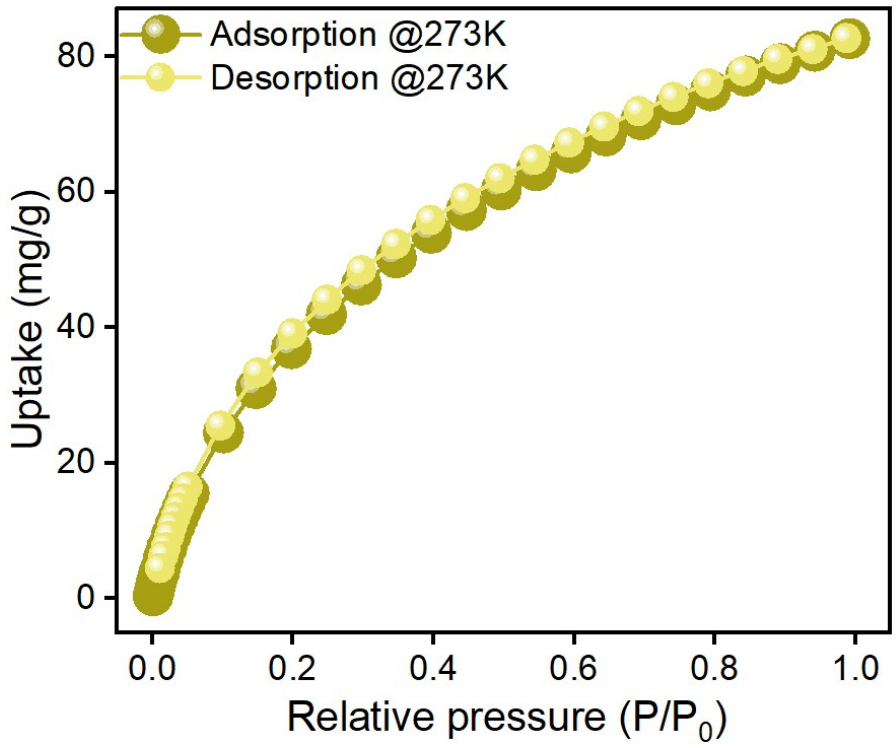

Figure S3: CO_2 sorption isotherm of Bi-Thio HCP at 273 K

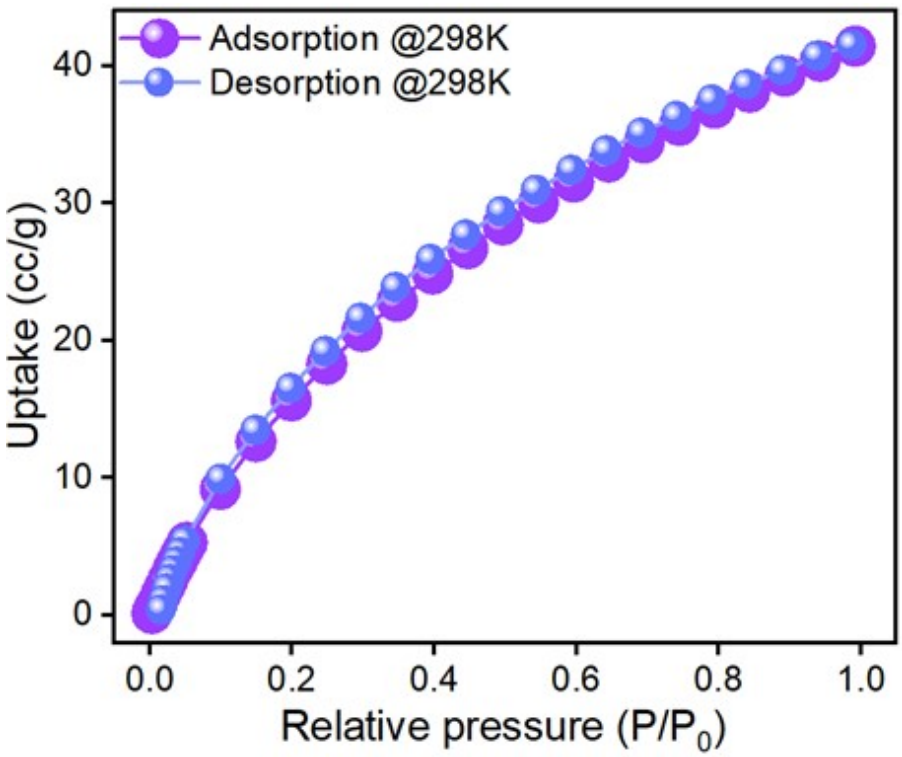

Figure S4: CO_2 sorption isotherm of Bi-Thio HCP at 298 K

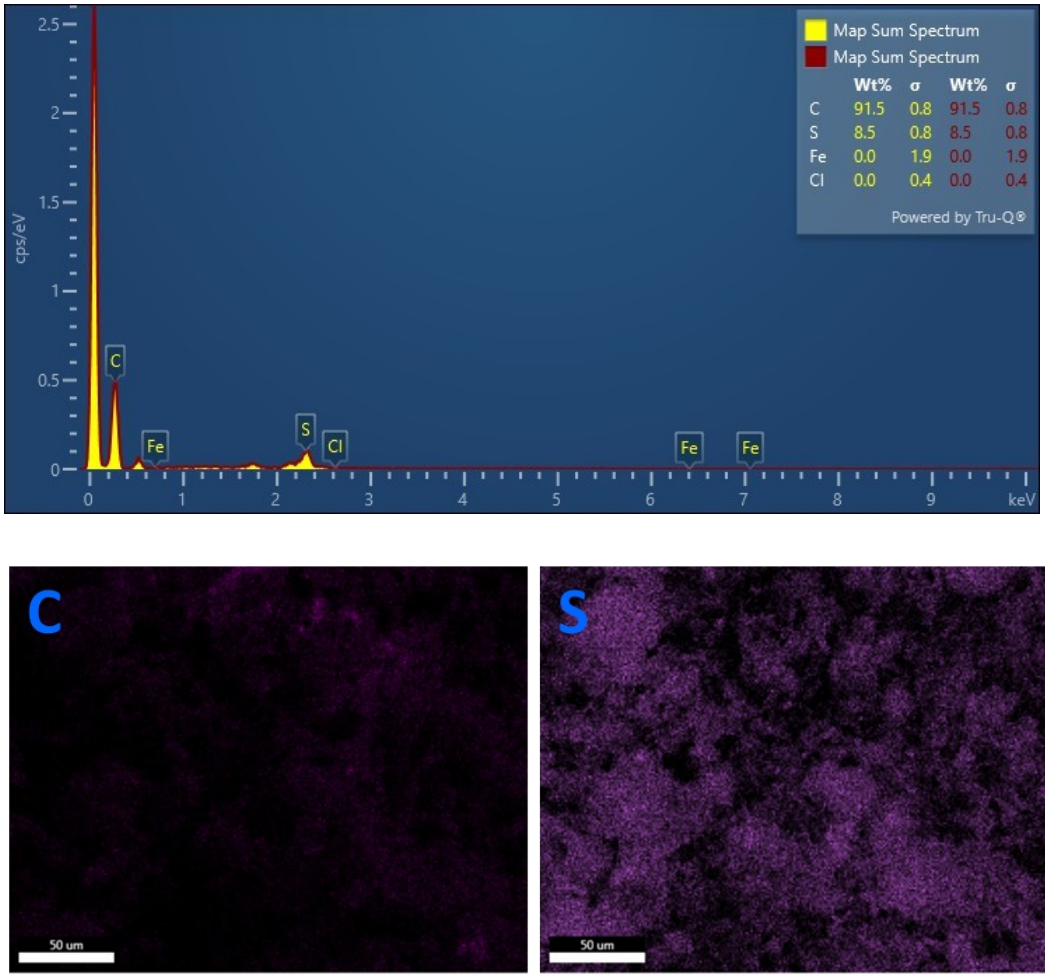

Figure S5: EDAX analysis and Elemental mapping of Bi-Thio HCP

Elements	Carbon (C)	Hydrogen (H)	Sulfur (S)
Weight (%)	66.06	3.26	22.86

Figure S6: CHNS analysis of the Bi-Thio HCP

Section-3

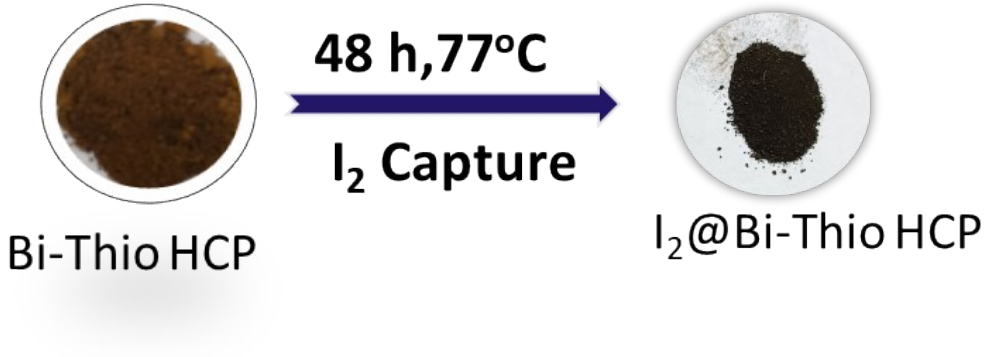

Figure S7: Digital images of the Bi-Thio HCP before and after iodine capture

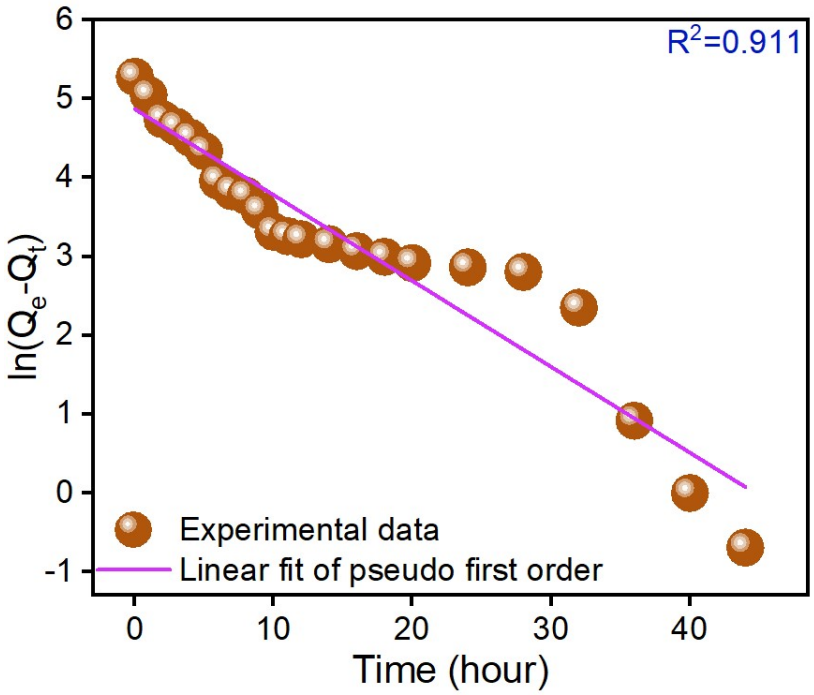

Figure S8: Pseudo first order kinetics plot of Bi-Thio HCP for iodine vapor uptake

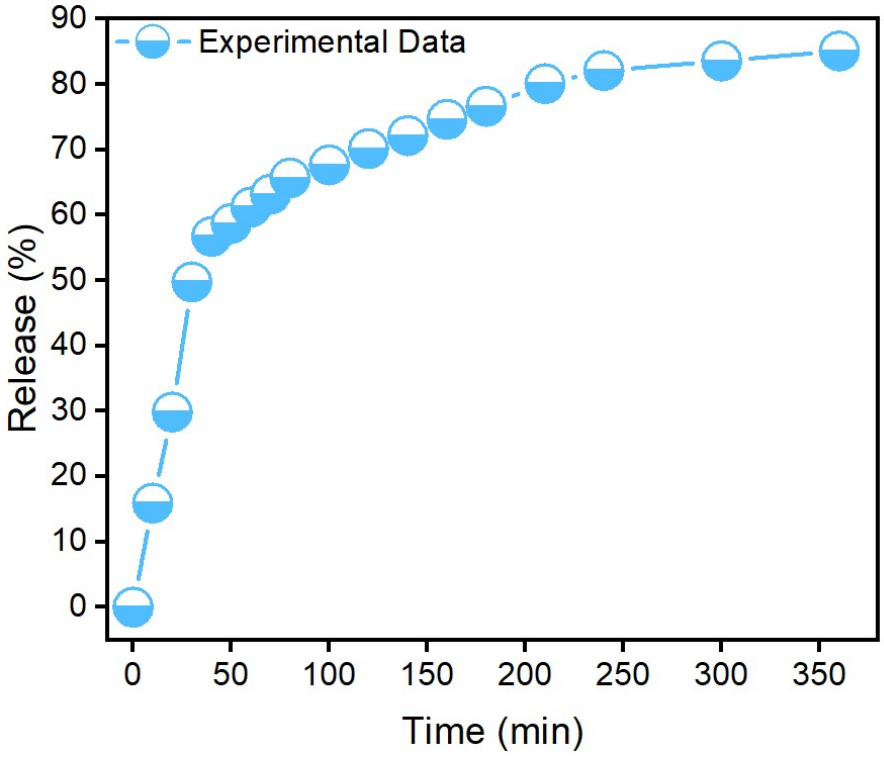

Figure S9: Iodine release of I_2@ Bi-Thio HCP upon heating at 125°C.

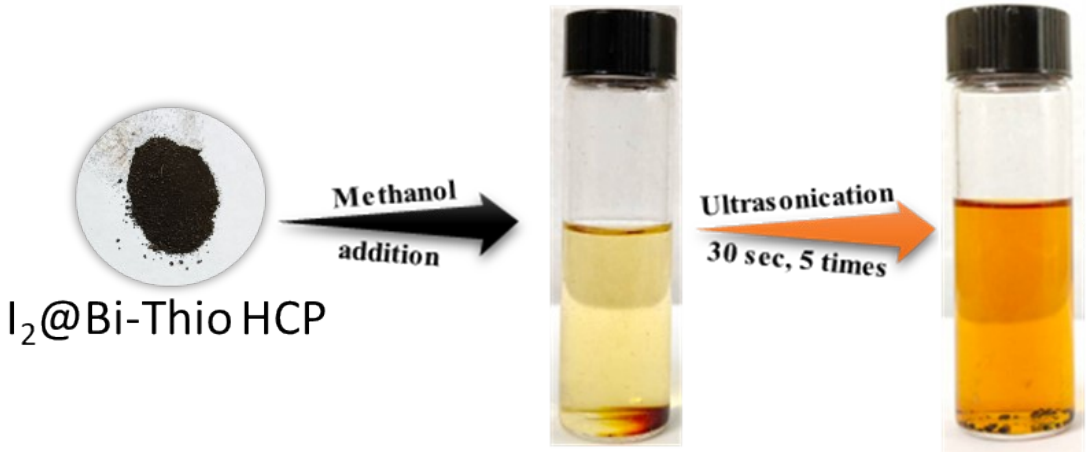

Figure S10: Digital images showing the iodine release in methanol from sample I_2 @Bi-Thio HCP

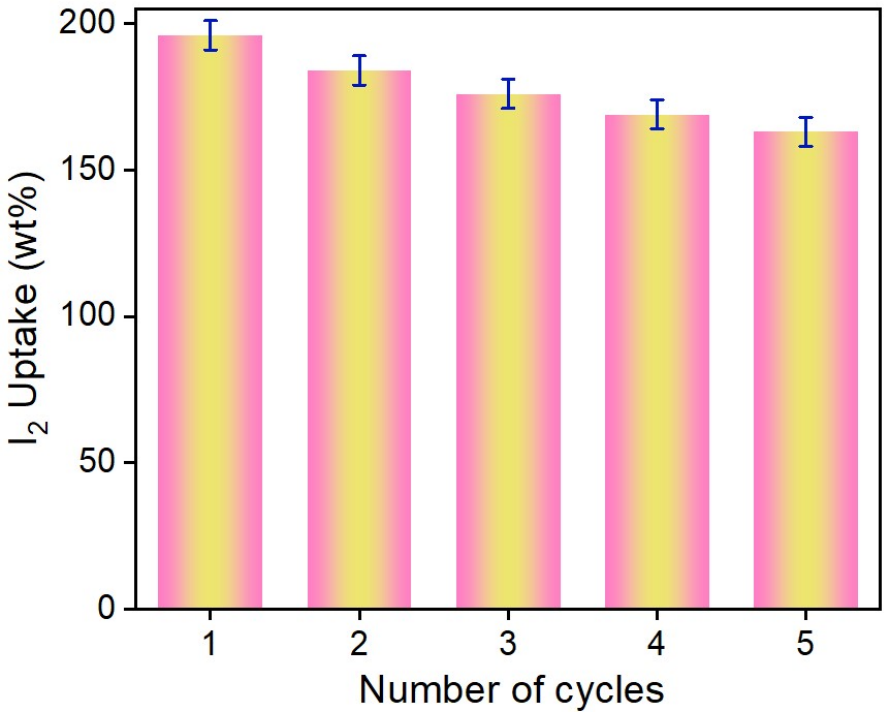

Figure S11: Iodine capture of recycled adsorbent Bi-Thio HCP over five cycles

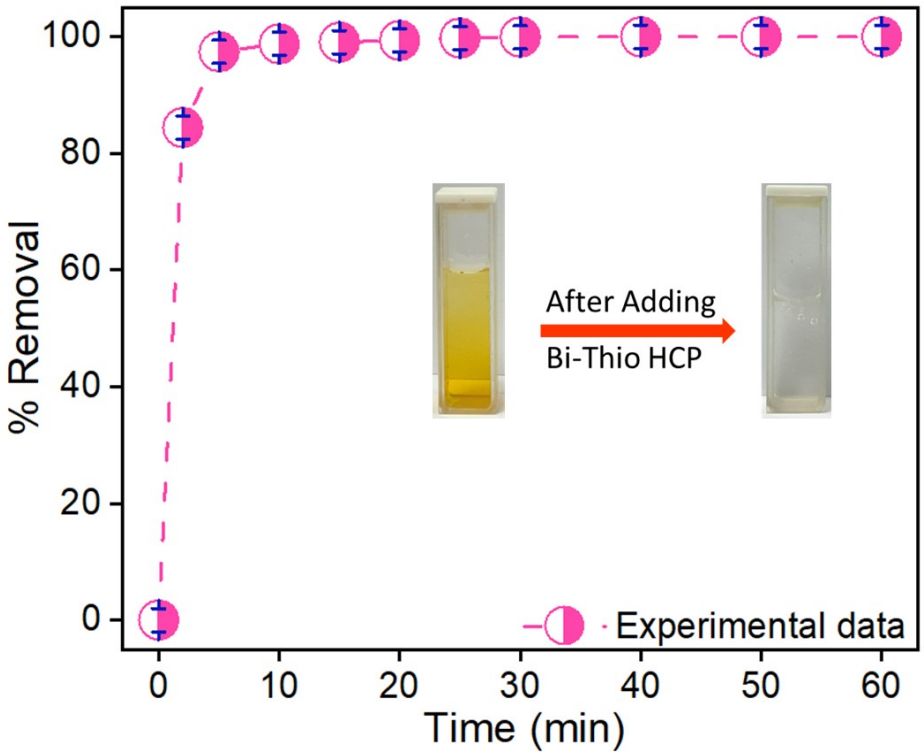

Figure S12: Removal efficiency of I_3^- with time by Bi-Thio HCP

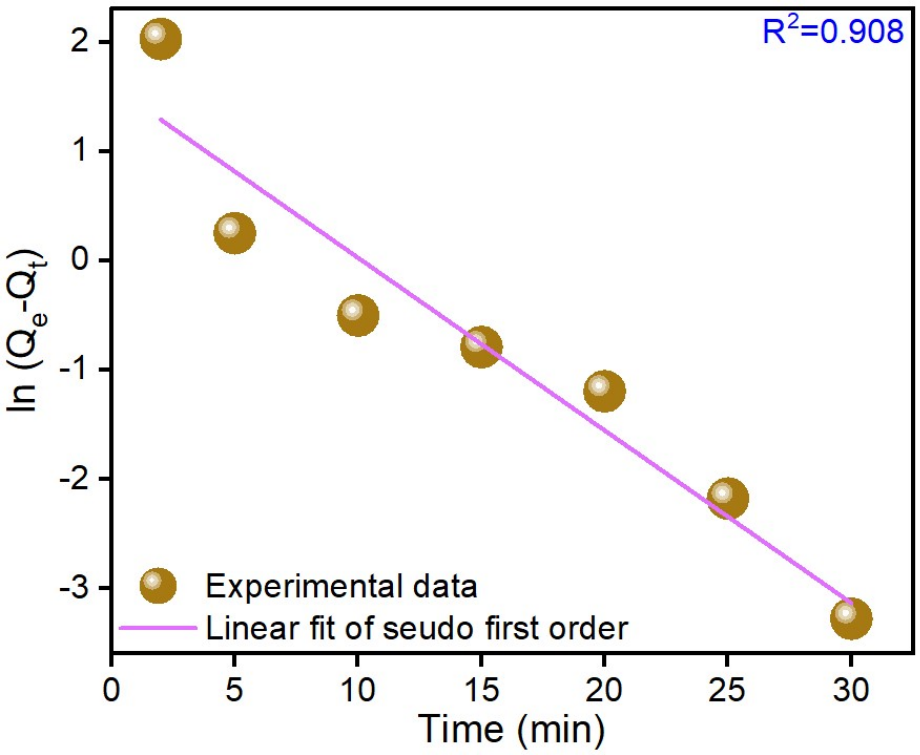

Figure S13: Pseudo first order kinetics plot of Bi-Thio HCP for I_3^-

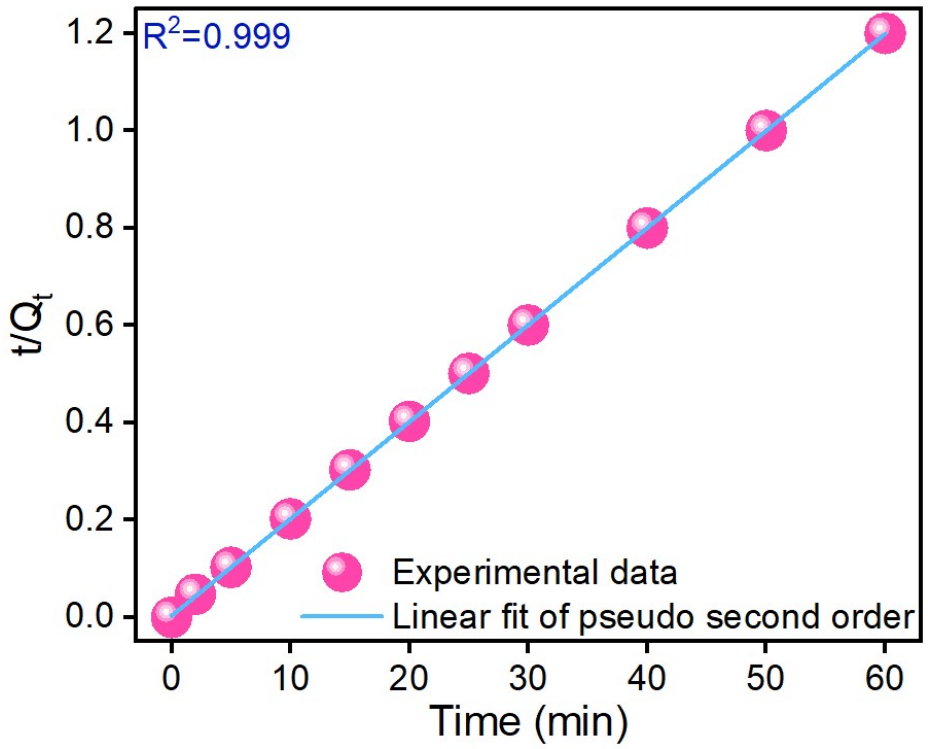

Figure S14: Pseudo second order kinetics plot of Bi-Thio HCP for I_3^-

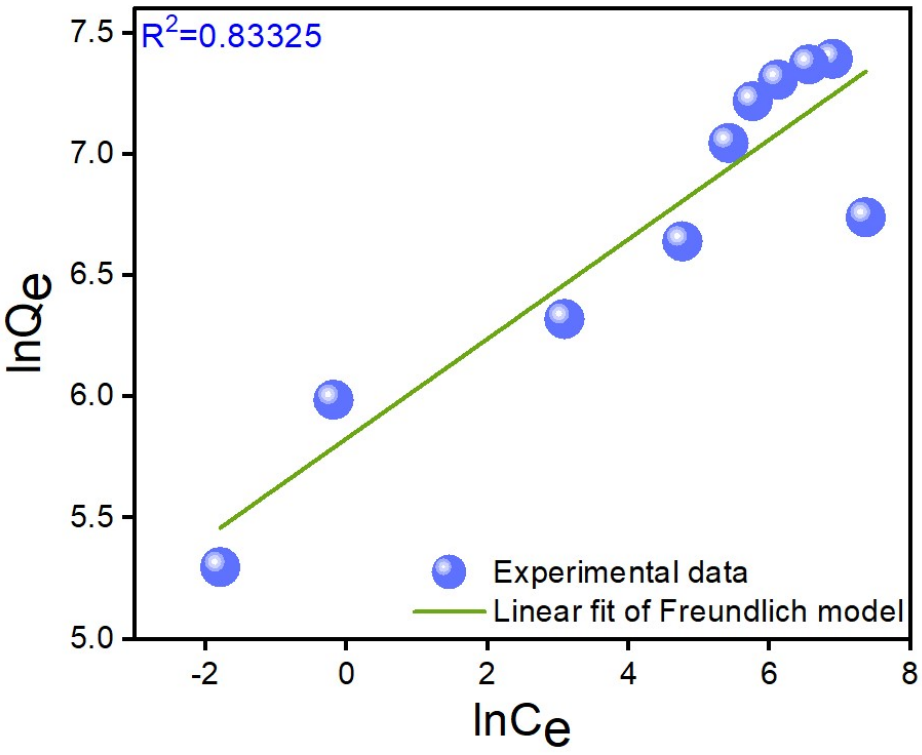

Figure S15: Freundlich isotherm model of Bi-Thio HCP for I_3^-

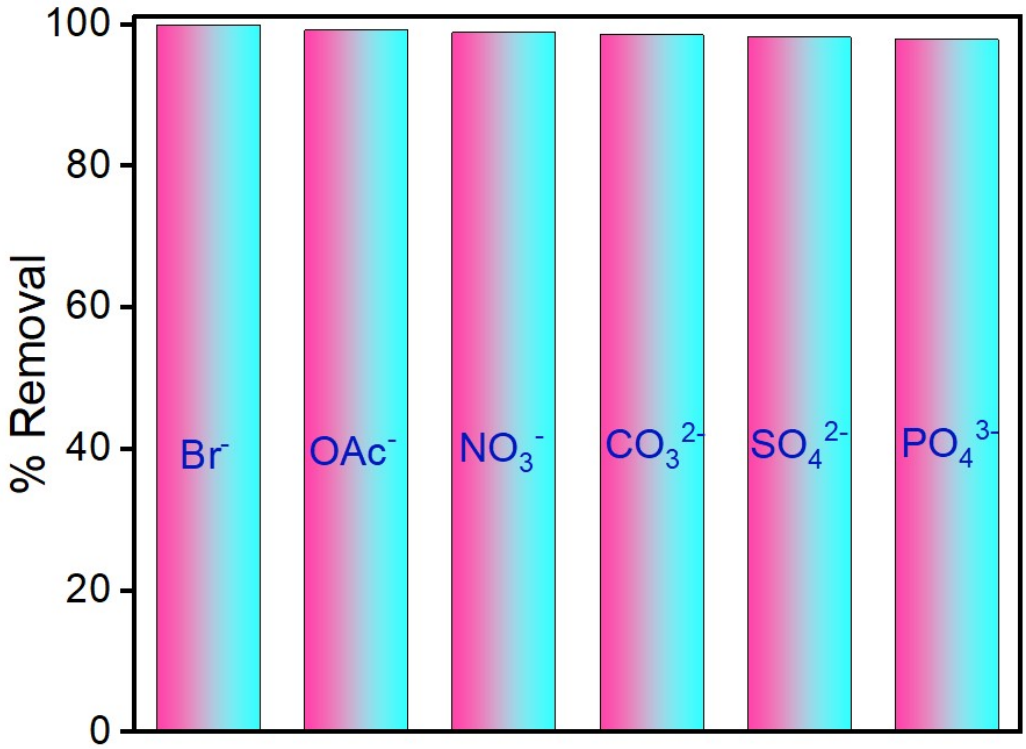

Figure S16: % Removal for I_3^- in aqueous solutions containing (1:1 equivalents) of different interfering anions together in the presence of Bi-Thio HCP

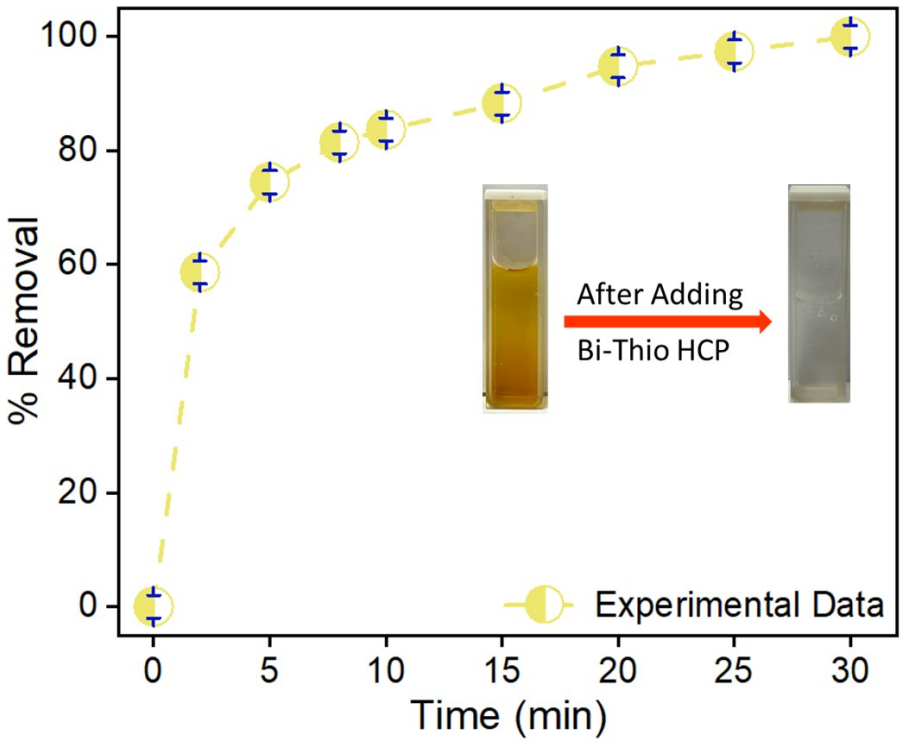

Figure S17: % Removal of I_2 in water with time by Bi-Thio HCP

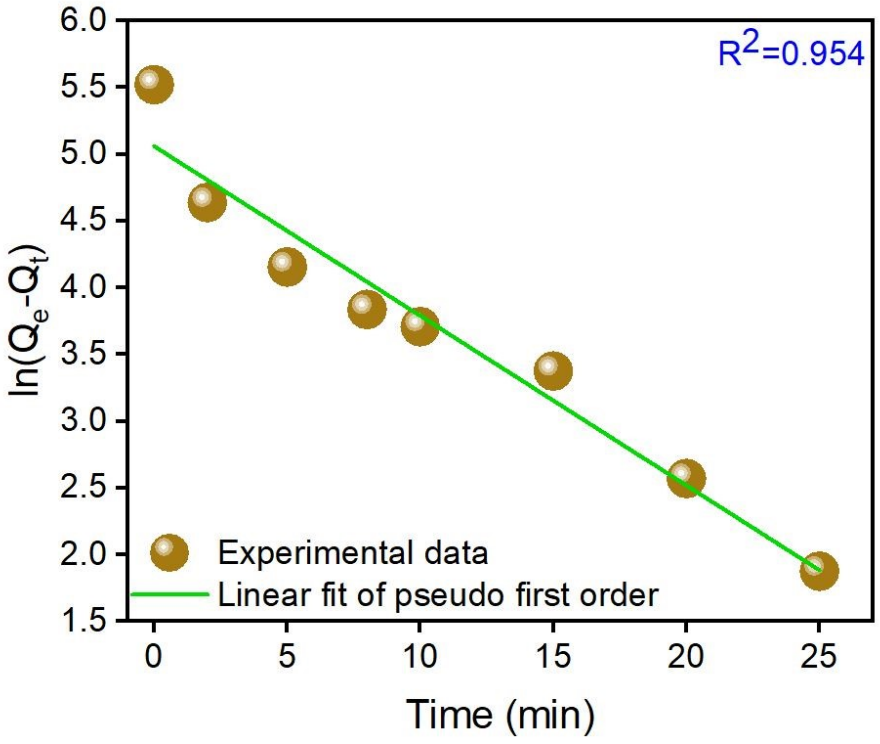

Figure S18: Pseudo first order kinetics plot of Bi-Thio HCP for I_2 in water

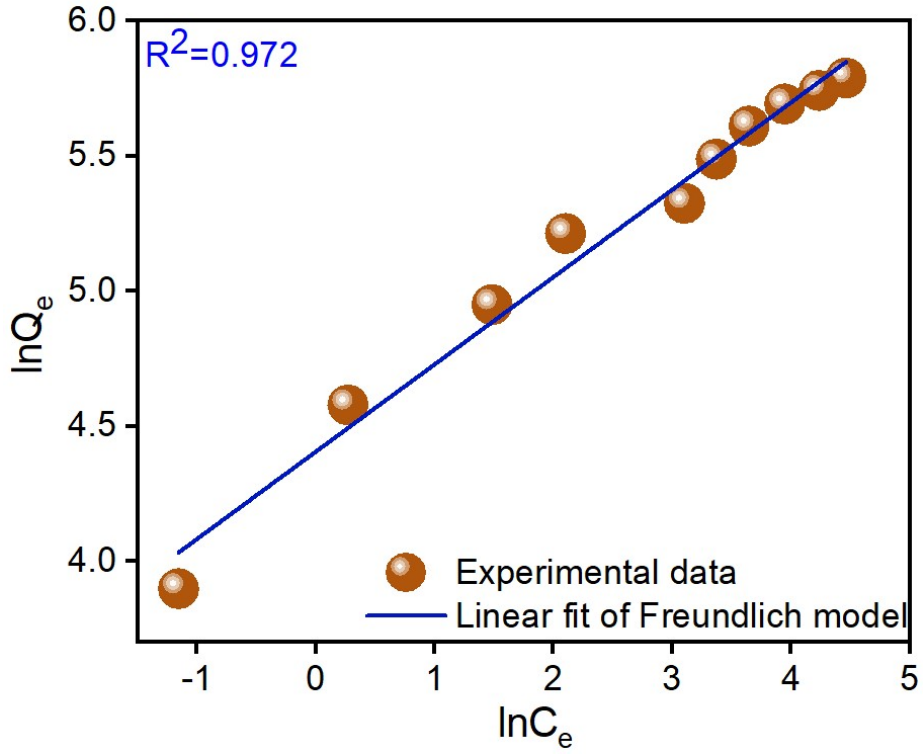

Figure S19: Freundlich isotherm model of Bi-Thio HCP for I_2 in water

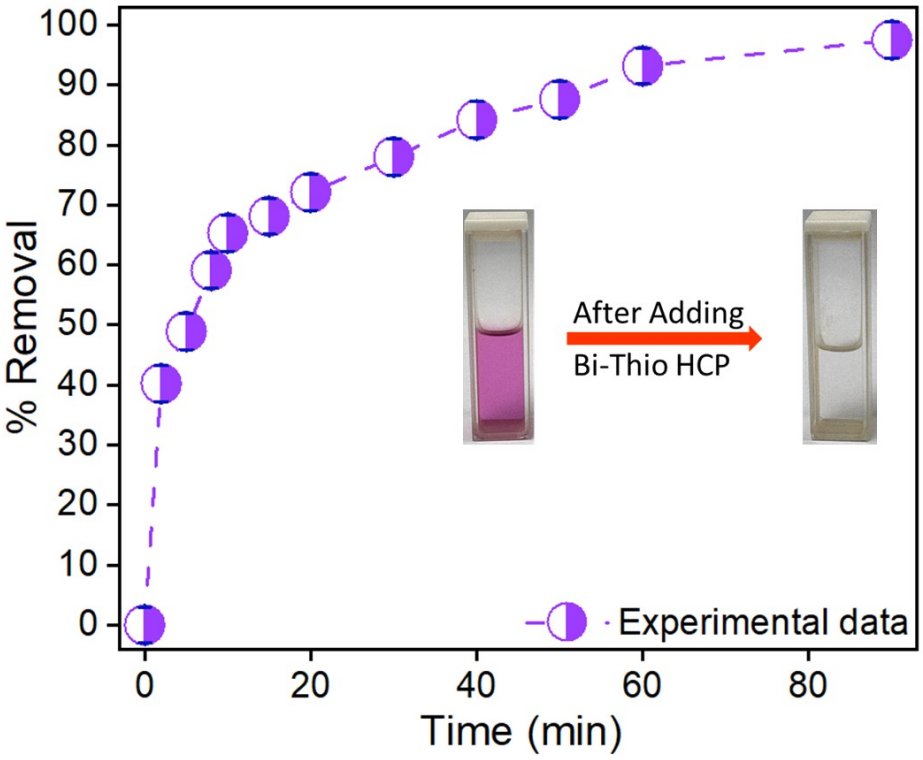

Figure S20: % Removal of I_2 in n-hexane with time by Bi-Thio HCP

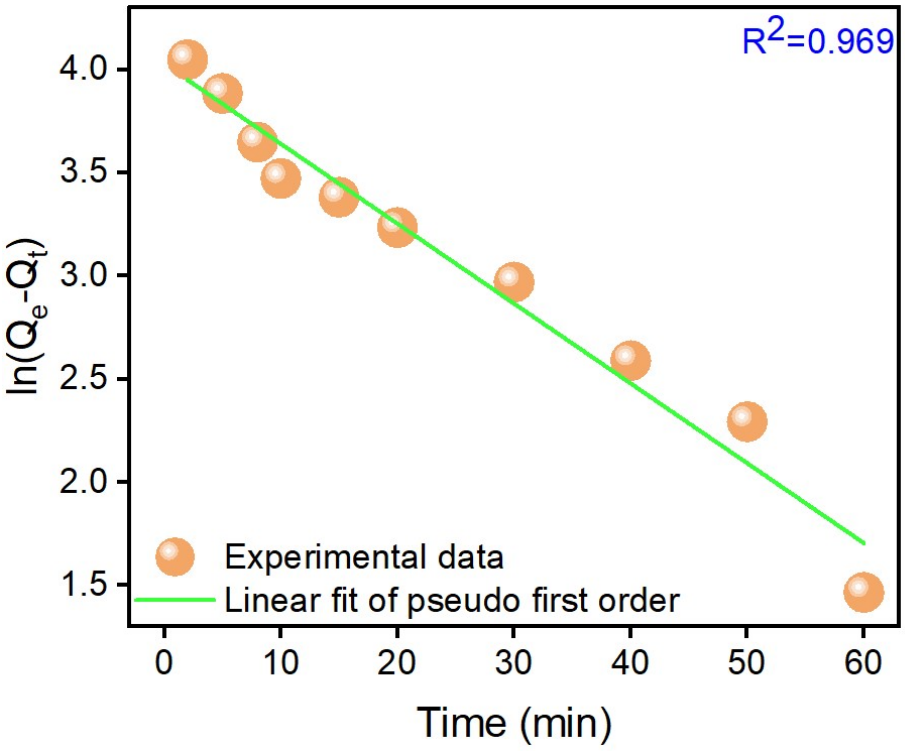

Figure S21: Pseudo first order kinetics plot of Bi-Thio HCP for I_2 in n-hexane

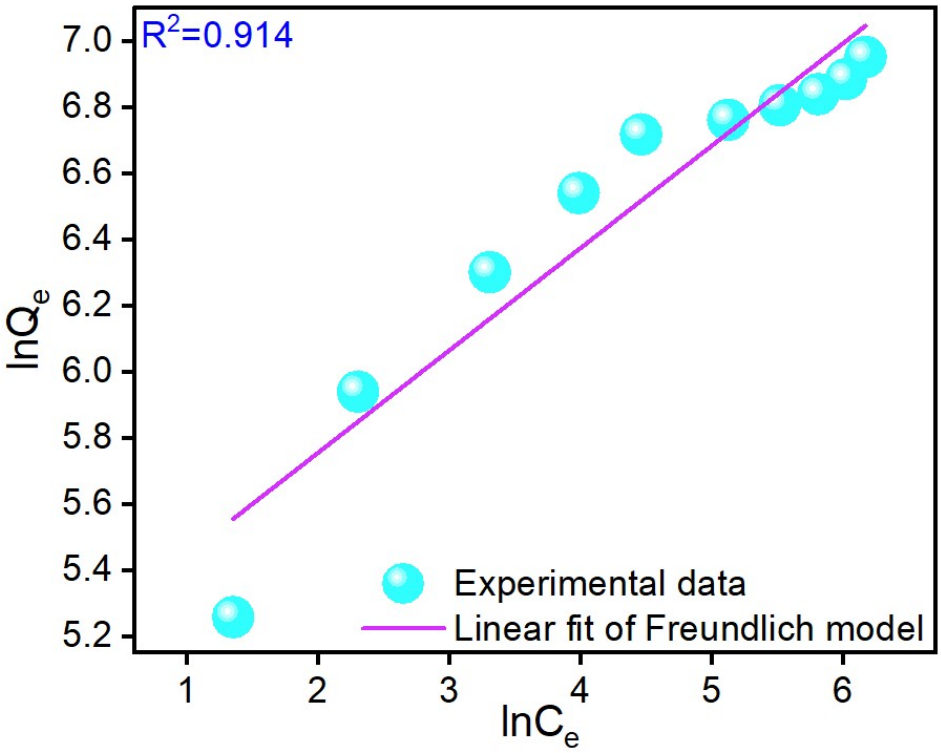

Figure S22: Freundlich isotherm model of Bi-Thio HCP for I_2 in n-hexane

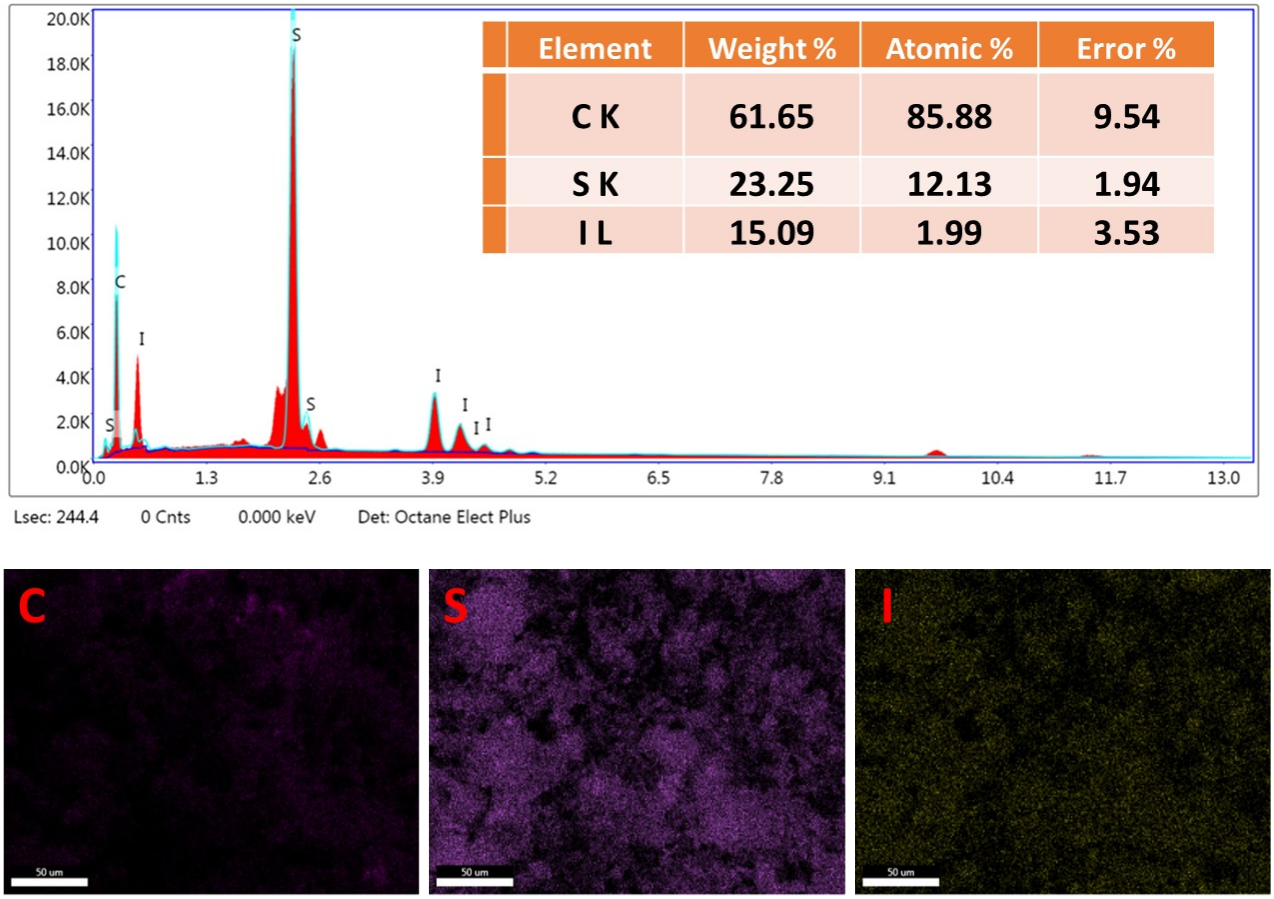

Element	Weight %	Atomic %	Error %
C K	61.65	85.88	9.54
S K	23.25	12.13	1.94
I L	15.09	1.99	3.53

Figure S23: EDAX and Elemental mapping of I_2@Bi-Thio HCP

Table S1: Comparing iodine adsorption by Bi-Thio HCP from the vapor phase with other POPs

Adsorbents	BET Surface area (m^2/g)	I_2 uptake (g/g)	Temperatures (°C)	Reference
Bi-Thio HCP	**664.10**	**1.96**	**77**	**This Work**
CMP-3	284.6	1.31	75	Angew. Chem. Int. Ed. **2021**, 60, 8967– 8975.
Cage-1	137	1.42	75	Chem. Commun**. 2020**, 56, 2491-2494.
CBP1	3.0	1.45	80	Polym. Chem. **2021**, 12, 2282-2292.
PAN-TPDA	752.0	1.45	72	Ind. Eng. Chem. Res. **2020**, 59, 3269-3278.
NM-COF-300	1374	1.48	75	J. Am. Chem. Soc. **2023**, 145, 4, 2544–2552
CMP-1	16.1	1.51	75	Angew. Chem., Int. Ed. **2021**, 60, 8967– 8975
CMP-2	20.2	1.77	75	Angew. Chem., Int. Ed. **2021**, 60, 8967– 8975
NRPP-1	1579	1.92	80	ACS Appl. Mater. Interfaces, **2018**, 10, 16049-16058
CPP 2	NR	2.00	80	Polym. Chem., **2020**, 11, 3066-3074
CMP-4	9.5	2.08	75	Angew. Chem., Int. Ed. **2021**, 60, 8967– 8975,
PAN-FPP5	788.0	2.22	72	Ind. Eng. Chem. Res. **2020**, 59, 3269-3278
NRPP-2	1028	2.22	80	ACS Appl. Mater. Interfaces, **2018**, 10, 16049-16058
TpPa-1	765	2.45	77	J. Solid State Chem. **2019**, 279, 120979
COF-TpgDB	210	2.75	75	ACS Omega **2020**, 5, 24262-24271
P-Am	1.262	2.83	85	ACS Appl. Polym. Mater. **2024**, *6,* 12, 7124–7136
$CMPNH_2$	6.44	2.83	75	J. Mater. Chem. A. **2020,** 8, 1966-1974
Micro-COF-1	816	2.9	75	Ind. Eng. Chem. Res. **2019,** 58, 10495-10502
HCP@Py-1	564.57	3.06	75	Chem. Eng. J. **2025**, *525*, 170103
PAN-T	1273	3.11	75	Polymer, **2020**, 194, 122401
Bpy-Cage	1.8	3.23	75	J. Am. Chem. Soc. **2022,** 144, 113-117
C[4]P-BTP	20.5	3.38	75	Angew. Chem. Int. Ed. **2022**, 61, e20211372

BisImiPOP@5	15.46	3.57	77	ACS Appl. Polym. Mater. **2021**, 3, 1, 354–361
OMC3	80	3.78	77	Angew. Chem. Int. Ed. **2020**, 59, 20846-20851
POP-2	41	3.82	80	J. Hazard. Mater. **2017**, 338, 224–232
COF-320	2400	4.0	75	Ind. Eng. Chem. Res. **2019**, 58, 10495-10502.
CalPOF-2	154	4.06	75	ACS Sustain. Chem. Eng. **2018**, 6, 17402– 17409
TTDP-3	13.20	4.25	75	ACS Appl. Polym. Mater. **2020**, 2, 5121– 5128
NDB-H	116.93	4.43	75	Chem. Asian J. **2018**, 13, 2046–2053
TAPB-QOT COP	10	4.64	77	ACS Appl. Mater. Interfaces **2023**, 15, 15819-15831
CalPOF-1	303	4.77	75	ACS Sustain. Chem. Eng. **2018**, 6, 17402– 17409
T_COP–1	206	4.86	75	Chem. Eng. J. **2022**, 427, 130950.
TTA-TTB COF	1733	5.0	77	Adv. Mater. **2018**, 30, 1801991.

Table S2: Comparing I_3^-adsorption from aqueous medium by Bi-Thio HCP with other POPs

Analyte	Name of Adsorbate	Capacity (mg/g)	References
I_3^-	**Bi-Thio HCP**	**1663.34**	**This Work**
I_3^-	MOF, KQ-1	131.5	J. Environ. Chem. Eng. **2021,** *9*, 106720.
I_3^-	Cadmium(II)-triazole MOF	180	*Chem. Commun.* **2011**, 47, 7185-7187.
I_3^-	BEPAFs	389.9	Sep. Purif. Technol. **2025,** 353**,** 128506.
I_3^-	NTP	429	ACS Macro Lett. **2016**, *5*, 1039-1043.
I_3^-	NiTi-S_x-LDH	527.40	Chem. Eng. J. **2019**, 378, 12218.
I_3^-	PAN-FPP5	700	Ind. Eng. Chem. Res. **2020**, *59*, 7, 3269–3278.
I_3^-	{[Zn_3(dllac)$_2$(pybz)$_2$]·2.5DMF}n (lac-Zn)	755	Sep. Purif. Technol. **2021**, *274,* 118436.
I_3^-	TCNQ-MA CTC	800	J. Hazard. Mater. **2024**, 465, 133488.
I_3^-	NOP-54	890	Chem. Eng. J. **2018**, *334*, 900-906.

I_3^-	Sil@NP	957.58	*J. Mater. Chem. A* **2015**, *3*, 179-188.
I_3^-	iPOP-6	1021	Soft Matter **2024**, *20*, 7832-7842.
I_3^-	NT-POP@800-2	1191	Sci. Rep. **2018**, *8*, 1867.
I_3^-	Keto-POP	1214	ACS Appl. Polym. Mater. **2025**,*7*, 8, 5127–5137.
I_3^-	UiO-66-PYDC	1240	Dalton Trans. **2017**, *46*, 7412-7420.
I_3^-	HCP[$H_{200}P_3$]	1388	ACS Appl. Polym. Mater. **2025,** *7*, 1639−1650.
I_3^-	iCON-4	1632.17	RSC Sustain.**2023***, 1,* 511-522.
I_3^-	HCP@Py-1	1790	Chem. Eng. J. **2025**, *525*, 170103.
I_3^-	TIEPE-DABCO	1800	Small **2023**, *19*, 2302902.
I_3^-	COF-TCO	2480	ACS Materials Lett. **2023**, *5*, 2422−2430.
I_3^-	HcOF-C1	2900	J. Am. Chem. Soc. **2017**, *139* 21, 7172–7175.
I_3^-	IT-Cage	2960	Langmuir **2024**, *40*, 11, 5959–5967.
I_3^-	BTPA-TTA-impyr-CF_3COOH	3170	Small **2024**, *20*, 2404994.

Section-4

Theoretical calculations for iodine adsorption in Bi-Thio HCP network:

The density functional theory (DFT) methodology with the B3LYP function was used to optimize the single repeating unit of Bi-Thio HCP and I_2, I_3^-, adsorbed structure of Bi-Thio HCP using a basis set of 6-311G (d,p) or SDD[1, 2]. For publication, Hartree-Fock (HF) energies have been estimated and converted to kJ/mol. Based on its ground state electron density, the electrostatic potential (ESP) on the surfaces of Bi-Thio HCP single repeating units. All of the abovementioned computations were carried out by using the Gaussian 16 software. The Multiwfn software was used to do the quantitative analysis using the Gaussian output wavefunction (.fch) files as inputs. The electron charge distribution for the interactions between Bi-Thio HCP and iodine was examined using the quantum theory of "atoms in molecules" (QTAIM). Three spatial coordinates (x, y, and z) could be thought of as multivariable functions of the electron density, where red indicates the presence of a force that repels atoms or molecules, and blue indicates strong adsorption. Gnuplot software is used to create RDG visualizations using the output file of the corresponding calculation, and Irfanview software is used to color the plot. These are commonly used programs for determining the QTAIM values and RDG plot for theoretical calculations.

The interaction energy of Bi-Thio HCP, I_2@Bi-Thio HCP and I_3^-@Bi-Thio HCP were calculated from this formula:

$$\Delta E = E_{\text{(Bi-Thio HCP +Iodine species)}} - E_{\text{(Bi-Thio HCP)}} - E_{\text{(Iodine species)}}$$

Where, $E_{\text{(Bi-Thio HCP +Iodine species)}}$ means optimized energy after adsorbed iodine species, $E_{\text{(Bi-Thio HCP)}}$ means optimized energy of Bi-Thio HCP alone, and $E_{\text{(Iodine species)}}$ means optimized energy of iodine species e.g. I_2, I_3^-.

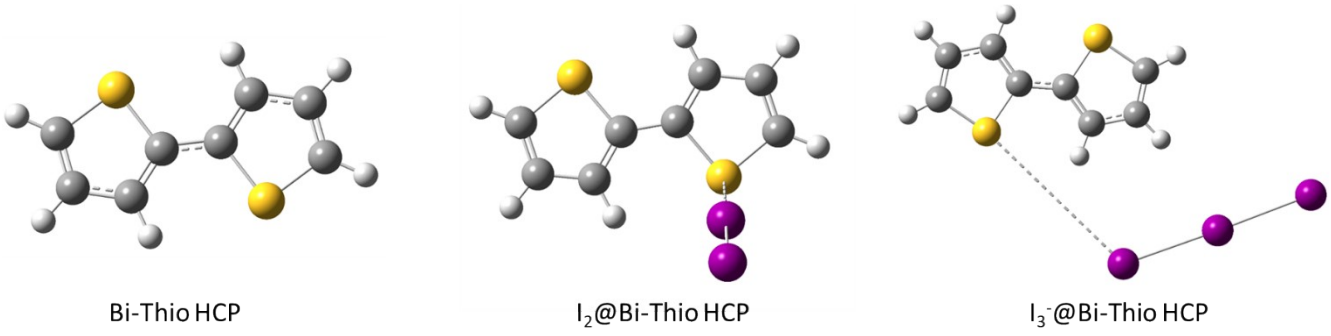

Figure S24: Optimized diagram of Bi-Thio HCP, I_2@ Bi-Thio HCP and I_3^-@Bi-Thio HCP

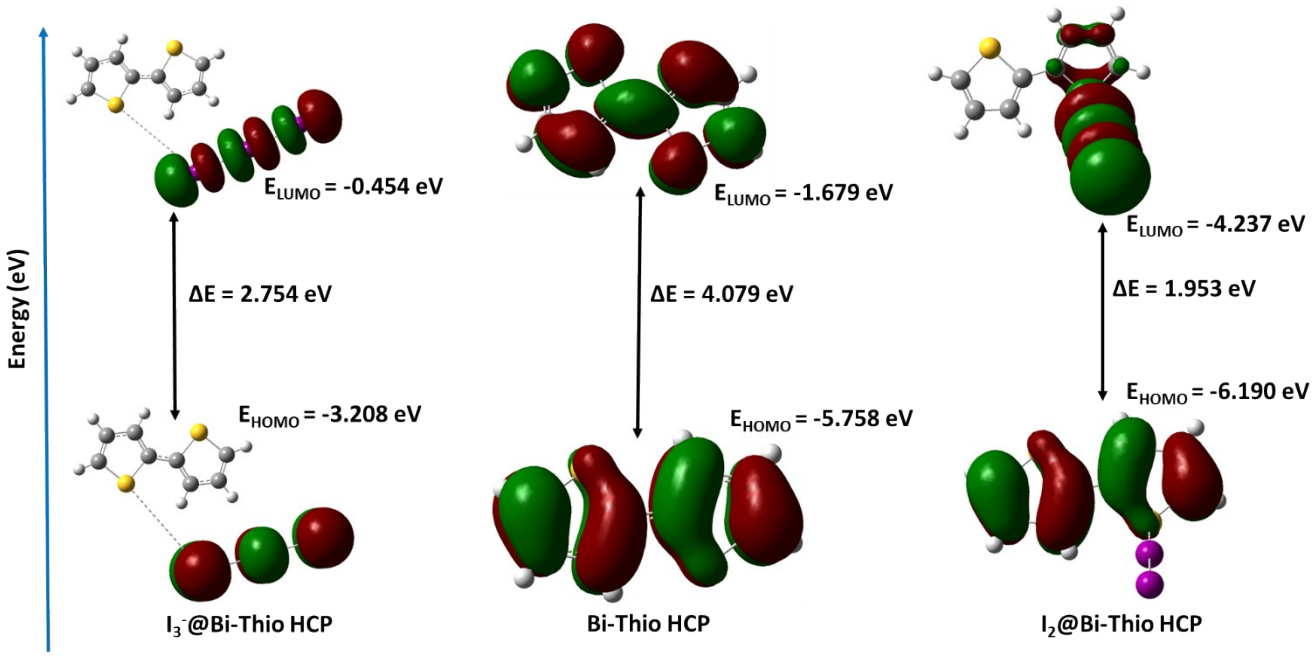

Figure S25: **HOMO-LUMO diagram with its energy of Bi-Thio HCP, I_2@ Bi-Thio HCP and I_3^-@Bi-Thio HCP**

Cartesian Coordinates-

(a) Cartesian Coordinates of Bi-Thio HCP:

Centre Number	Atomic Number	Atomic Type	X (Å)	Y(Å)	Z(Å)
1	6	C	-0.000049	0.719501	0.000003
2	6	C	1.049661	1.603013	0.000381
3	6	C	0.672081	2.983735	0.000118
4	6	C	-0.672081	3.191986	0.000034
5	16	S	-1.584872	1.635837	-0.000260
6	1	H	2.079217	1.276823	0.000682
7	1	H	1.389437	3.790879	0.000250
8	1	H	-1.223279	4.114715	0.000015

9	6	C	0.000049	-0.719501	0.000003
10	6	C	-1.049661	-1.603013	0.000381
11	16	S	1.584872	-1.635837	-0.000260
12	6	C	-0.672081	-2.983735	0.000118
13	1	H	-2.079217	-1.276823	0.000682
14	6	C	0.672081	-3.191986	0.000034
15	1	H	-1.389437	-3.790879	0.000250
16	1	H	1.223279	-4.114715	0.000015

(b) Cartesian Coordinates of I_2@Bi-Thio HCP:

Centre Number	Atomic Number	Atomic Type	X (Å)	Y(Å)	Z(Å)
1	6	C	2.578242	0.882462	0.000398
2	6	C	3.154661	2.137609	-0.000222
3	6	C	2.169429	3.182320	-0.000734
4	6	C	0.885934	2.679380	0.000275
5	16	S	0.882637	0.983423	0.001123
6	1	H	4.226654	2.331643	-0.000548
7	1	H	2.425075	4.241081	-0.001807
8	1	H	-0.029276	3.263847	0.000592
9	6	C	3.322163	-0.445609	0.000385
10	6	C	2.742196	-1.700611	0.001015
11	16	S	5.013658	-0.541193	-0.000538
12	6	C	3.727768	-2.742847	0.000075

13	1	H	1.670397	-1.896886	0.001864
14	6	C	5.011060	-2.233695	-0.000469
15	1	H	3.474174	-3.802109	-0.000174
16	1	H	5.926387	-2.817689	-0.000745
17	53	I	-3.691073	-0.562420	-0.000117
18	53	I	-1.093509	0.204880	-0.000126

(c) Cartesian Coordinates of I_3^- @Bi-Thio HCP:

Centre Number	Atomic Number	Atomic Type	X (Å)	Y(Å)	Z(Å)
1	6	C	-4.758635	-0.474213	-0.162401
2	6	C	-5.299081	-1.260187	-1.175782
3	6	C	-4.933916	-2.637690	-1.090043
4	6	C	-4.118612	-2.916222	-0.006325
5	16	S	-3.742618	-1.468755	0.959327
6	1	H	-5.930561	-0.861840	-1.965920
7	1	H	-5.260374	-3.386448	-1.806084
8	1	H	-3.683047	-3.856499	0.297448
9	6	C	-4.909471	0.943550	0.072944
10	6	C	-4.303468	1.745724	1.022789
11	16	S	-6.017646	1.948112	-0.967832
12	6	C	-4.686947	3.134027	0.961343
13	1	H	-3.585728	1.357405	1.736433
14	6	C	-5.592729	3.420880	-0.035050
15	1	H	-4.289250	3.886734	1.634243

16	1	H	-6.037025	4.368009	-0.306228
17	53	I	2.596963	-0.172523	-0.123664
18	53	I	-0.498138	-0.825912	0.309251
19	53	I	5.760937	0.603863	-0.128580

References:

1. A. Hassan, R. K. Pandey, A. Chakraborty, S. A. Wahed, T. R. Rao and N. Das, Soft Matter, 2024, 20, 7832-7842.
2. A. Hassan, S. Mondal, S. A. Wahed, S. Goswami, A. Alam, M. Ghosh, K. K. Dey and N. Das, ACS Applied Nano Materials, 2025, 8, 12895-12908.